Diurnal Variation of Atmospheric Pollutant Concentrations Affected by Development of Windstorms along the Lee Side of Coastal Mountain Area

Hyo Choi

Dept. of Atmospheric Sciences, Kangnung National University, Kangnung, Kangwondo 210-702, Korea

(Manuscript received 15 November 1996)

Abstract

Before (March 26. 1994) or after the occurrence of a downslope windstorm (March 29), the NO, NO_2, and SO_2 at the ground level of Kangnung city were monitored with high concentrations in the afternoon, due to a large amount of gases emitted from combustion of motor vehicle and heating apparatus, especially near 1600-1800 LST and 2000-2100 LST, but at night, they had low concentrations, resulting from small consumptions of vehicle and heating fuels. When both moderate westerly synoptic-scale winds flow over Mt. Taegwallyang and easterly meso-scale sea breeze during the day, atmospheric pollutants should be trapped by two different wind systems, resulting in higher concentration at Kangnung city in the afternoon. At night, the association of westerly synoptic wind and land breeze can produce relatively strong winds and the dissipation by the winds cause these low concentrations to lower and lower, as nightime goes on.

From March 27 through 28, an enforced localized windstorm could be produced along the lee side of the mountain near Kangnung, generating westerly internal gravity waves with hydraulic jump motions. Sea breeze toward inland appartantly confines to the bottom of the eastern side of the mountain, due to the interruption of eastward violent internal gravity waves. As the windstorm moves down toward the ground, an encountering point of two opposite winds approaches Kangnung, and a great amount of NO and NO_2 were removed by the strong surface winds. Thus, their

maximum concentrations are found to be near 18 and 20 LST. 17 and 21 LST. In the nighttime. the more developed storm should produce very strong surface winds and the NO and NO_2 could be easily dissipated into other place. The SO_2 concentration had no maximum value. that is. almost constant one all day long. due to its removal by the strong surface wind. Especially. the CO concentrations were slightly lower during the strom period than both before or after the strom. but they were nearly constant without much changes during the daytime and nighttime.

1. Introduction

In the recent years. many environmental scientists have explained atmospheric pollutant concentrations such as NO. NO_2 and SO_2 through measurement and numerical modelling [*Kimura*. 1983; *Leighton*. 1961; *Perkins*. 1974; *Stephene*. 1969a and 1969b] . Choi and Choi (1995) demonstrated diurnal variations of TSP and O_3 concentrations under the influence of internal gravity waves. Diurnal variations of NO (nitric oxide). NO_2 (nitrogen dioxide) SO_2 (sulfur dioxide) and CO (carbon monoxide) concentrations under the development of downslope windstorm and see-land breeze circulations in the mountainous coastal region of Korea show different patterns compared with their typical variations in spring. Since the daytime heating rate in the lower atmosphere at the ground surface of a mountain is greater than that over a plain and sea on a clear and calm day. the accumulated warmer air at the ground surface of the mountain induces a surface pressure depression during the daytime (Kuwagata and Sumioka. 1991). The daytime atmospheric pressure difference between the mountain and coastal sea can generate a surface wind. which flows from the sea to the mountain. although the seperating mountain range may act as a barrier to suppress such a wind system. This surface winds should therefore depend upon the topographic features and atmospheric conditions [*Choi and Choi*. 1994; *Choi and Choi*. 1995; *Pielke*. 1984] . The topographical effect on the heating rate causes that the temperature of the lower atmosphere in the mountain increases more than over the plain and coastal sea [*Friehe and Winant*. 1982; *Hsu*. 1979. 1980 and 1988)]

Davies [1987] . *Hsu* [1980. 1988] . *Lilly et al.* [1982] . *McPherson* [1970] . *Plate* [1971] . *Raynor et al.* [1979] . *SethuRaman* [1982] and *Taylor* [1970] insisted that atmospheric circulations near the mountainous coastal seas can be affected by both orographic effects and sea breeze phenomena and influence upon atmospheric pollutant concentrations. Numerical simulations on downslope windstorms with development of internal gravity waves were carried out by *Peltier and Clark* [1979] . *Satomura and Bougeault* [1992] . *Smith* [1978. 1989] . *WMO* [1986] and *Smolarkiewicz and Rotunno* [1989] .

Kangnung city in the mountainous coastal region often record unusal levels of air pollution [*WREA*. 1994] . In the present study. we describe the transportations and variations of atmospheric pollutants in the coastal mountainous region. under the influence of windstorms.

2. Data analysis and numerical method

Under the mentioned wind system above, the particular regards were given to air quality analysis of NO, NO_2, SO_2 and CO. Hourly data of those concentrations from 0100 LST on March 26 through 2400 LST on March 29, 1994 were automatically measured by DASBI-4108, DASBI-2108 and DASBI-2508, which were manufactured by DASBI company in U.S.A.. The dectors were established at the top of Ihmdang-dong office, Kangnung city and reanalyzed by Wonju Regional Environmental Administration [*WREA*, 1994] .

In our model domain, the study areas consist of complex terrains, where are characterized by forest in a high mountain called Mt. Whangbyung (1407m) in the west, buildings and apartments inside an urban area (Kangnung city) in the centeral part of the study area and sand beach near the sea in the east [*Choi and Choi*, 1995; Figs. 1 and 2] . A non-hydrostatic grid point model with one way double-nesting technique in a complex terrain-following coordinate was used to investigate the structure of wind storm, concerning about both development of internal gravity wave and sea breeze circulation in the coastal region for a 30 hour prediction experiment from 0900 LST (Local Standard Time = 9^h + Greenwich Mean Time), March 27 to 1200 LST, March 28 by using HITACH super computer established at Meteorological Research Institute, JMA. The grid domain consists of 34 x 34 grid points with a uniform horizontal interval as 20km in the coarse-mesh model and 7km in the fine-mesh for double nesting.

This model has 15 vertical levels from 10m to 6km over the ground, which are 10, 45, . . . 5400m with sequentially larger intervals. Through horizontal and vertical interpolations of 12 hourly global analysis data (G-ANAL) on winds, potential temperature, specific humidity produced by Japan Meteorological Agency (JMA), their initial data were provided for lateral boundary data in a coarse-mesh model and predicted values by the coarse-mesh model were used for a fine-mesh model. In order to find out how horizontal gradients of sea surface temperatures (SST) can enhance the surface winds over the sea, comparing to the effects of horizontal gradients of air temperatures over the inland and sea surfaces, the SST data obtained by NOAA (National Oceanic and Atmospheric Administration) satellite were used.

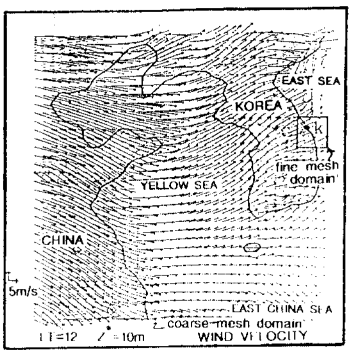

Fig. 1. Surface winds (m/s) at 10m height over the ground surface surrounding Korea at 12 LST, March 27, 1994 in a coarse -mesh domain of model. Box is a fine-mesh domain including Kangnung city.

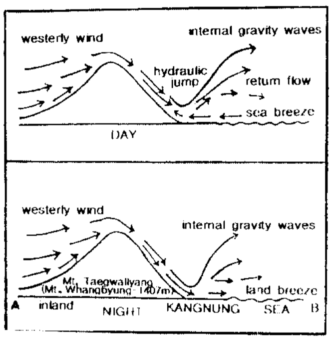

Fig. 2. Schematic profiles of air flows over the eastern mountainous coastal region for day and night during the windstorm period

3. Numerical model formulations

3.1. Basic equations

The model is based upon Boussinesq and anelastic approximations using a three - dimensional non-hydrostatical model in a terrain-following coordinate system [*Choi*, 1996; *Kimura and Takahashi*, 1991] . The equations of motion can be derived as

$$d_t hu = fhv - h\Theta\partial_x \Pi + \Theta(z_T - z^{\bullet})\partial_x z_G \partial_z \Pi + z_T^2/h\partial_z(K_m \partial_z u) \tag{1}$$

$$d_t hv = - fhu - h\Theta\partial_y \Pi + \Theta(z_T - z^{\bullet})\partial_y z_G \partial_z \Pi + z_T^2/h\partial_z(K_m \partial_z v) \tag{2}$$

$$d_t hw^{\bullet} = - z_T \Theta \partial_z \Pi + gh\theta/\Theta \tag{3}$$

$$\Theta = T(P_{00}/P)^{R_d/C_p} \tag{4}$$

where

$$\begin{aligned} z^{\bullet} &= z_T (z - z_G)/h \\ h &= z_T - z_G \\ d_t &= \partial_t + u\partial_X + v\partial_y + w^{\bullet}\partial_z \\ hw^{\bullet} &= z_T w + (z^{\bullet} - z_T)(\partial_x z_G u + \partial_y z_G v) \end{aligned} \tag{5}$$

where Θ, T, z, z_T, z_G and K_m imply potential temperature(K), air temperature at a given height, actual height, height of upper boundary with its change for time and place in a model domain, height of topography and vertical diffusion coefficient for momentum(m^2/s), respectively. g is gravity(m/s^2) and u, v, and $w^{\bullet}$ are velocity compoments in the x, y and z directions in the $z^{\bullet}$ coordinate. P, P_{00}, R, R_d, and C_p are atmospheric pressure, atmospheric pressure at reference level, universal gas constant, gas constant for dry air and specific heat at constant pressure. f is Coriolis parameter ($f=2\Omega\sin\varphi$, Ω: angular velocity of the earth rotation, φ: latitude).

From the thermodynamic equation and conservation of water vapor following equations for radiative heating of air yields to

$$d_t h\Theta = z_T^2/h\partial_z(K_h \partial_z \Theta) + hQ_r \tag{6}$$

$$d_t hq = z_T^2/h\partial_z(K_h \partial_Z q) \tag{7}$$

where Q_r and q are radiative heating rate of atmosphere and potential temperature and specific humidity of water vapor. In this model condensation processes are not considered.

The continuity equation is

$$\partial_x hu + \partial_y hv + \partial_z hw^{\cdot} = 0 \tag{8}$$

Assuming that horizontal scale of the phenomena is one order greater than vertical scale, Eq.(3) for hydrostatic and non-hydrostatic equilibrum cases can be converted into the following pressure equations as

For hydrostatic state

$$\partial_z \pi = h/z_T \; g/\Theta^2 \theta \tag{9}$$

For non-hydrostatic one

$$\Pi = \pi - \pi_H \tag{10}$$

$$\partial_z \pi_H = gh\theta/(\Theta^2 z_T) \tag{11}$$

$$\begin{aligned}
&\partial_{xx}\Pi + \partial_{yy}\Pi + \{(z_T/(z_T - z_G))^2 \\
&+ ((z^{\cdot} - z_T)/h)^2 \, ((\partial_x z_G)^2 + (\partial_y z_G)^2)\}\partial_{zz}\Pi \\
&+ 2(z^{\cdot} - z_T)/h \; \partial_x z_G \; \partial_{xz}\Pi \\
&+ 2(z^{\cdot} - z_T)/h \; \partial_y z_G \; \partial_{yz}\Pi \\
&+ \{(z^{\cdot} - z_T)/h \; (\partial_{xx} z_G + \partial_{yy} z_G) \\
&+ 2(z^{\cdot} - z_T)/h^2 \, ((\partial_x z_G)^2 + (\partial_y z_G)^2)\}\partial_z\Pi \\
&= r(x, y, z^{\cdot})/(\Theta h)
\end{aligned} \tag{12}$$

where the residual term, r is written by

$$\begin{aligned}
r(x, y, z^{\cdot}) = \; &\partial_x ADVX + \partial_y ADVY + z_T/h \; \partial_z ADVZ \\
&+ 1/h \; \partial_x z_G \partial_z (z^{\cdot} - z_T) ADVX \\
&+ 1/h \; \partial_y z_G \partial_z (z^{\cdot} - z_T) ADVY
\end{aligned} \tag{13}$$

and

$$\begin{aligned}
ADVX = \; &- \partial_x huu - \partial_y huv - \partial_z huw^{\cdot} + fhv \\
&- \Theta h \partial_x \pi_H - \Theta (z^{\cdot} - z_T) \partial_x z_G \; \partial_z \pi_H \\
&+ z_T^2/h \partial_z (K_m \partial_z u)
\end{aligned}$$

$$\begin{aligned}
ADVY = \; &- \partial_x huv - \partial_y hvv - \partial_z hvw^{\cdot} - fhu \\
&- \Theta h \partial_y \pi_H - \Theta (z^{\cdot} - z_T) \partial_y z_G \partial_z \pi_H \\
&+ z_T^2/h \partial_z (K_m \partial_z v)
\end{aligned}$$

$$ADVZ = - \partial_x huw - \partial_y hvw - \partial_z hww^{\cdot}$$

In order to calculate the solutions of Eqs. (1), (2), (6), and (7) for the time integration and the vertical direction in z^* coordinate, Euler-backward scheme and Crank-Nicholson scheme are adopted, respectively. The atmospheric pressure changes at the top of model atmosphere with a material surface (here, 6000m) were controlled by *Durran and Klemp* [1987] and *Klemp and Durran* [1983]'s wave radiative condition, avoiding reflection of gravity waves generated in the lower layers. The open boundary condition developed by *Orlanski* [1976] for u, v, θ and q was modified for the lateral boundary condition of the model domain. Since a small time interval is effective to reduce external gravity waves appearing in the equations, it was determined by Δt=30sec in this simulation.

In the surface boundary layer, the vertical diffusion coefficients, K_m and K_h for momentum and heat were evaluated from the turbulent closure level-2 model [*Mellor and Yamada*, 1974; *Yamada*, 1983; *Yamada and Mellor*, 1983]. Total net flux of long wave radiation absorbed by water vapor and carbon dioxide and flux from the ground surface toward the upper levels, which assumes to have a positive sign, considering H_2O and CO_2 transmission fuctions, effective vapor amount, specific humidity (g/cm^2), pressure (mb) at the surface and at the arbitrary levels. The solar radiation toward the earth surface, which has a positive flux and total net solar radiation at the ground, as a function of solar zenth angle, latitude, declination and time angle. Newtonian cooling due to long wave radiation, radiative heating rate for air and soil temperatures at the ground level was also consider in detail.

For energy budget in the surface boundary layer, the surface boundary layer such as 10m height over the ground was assumed to be a constant flux layer in order to eatimate the sensible and latent heat fluxes and the similarity theory is adopted [*Businger*, 1973; *Kimura and Takahashi*, 1991; *Monin*, 1970; *Panofsky and Dutton*, 1984; *Paulson*, 1970; *Williams*, 1980]. On the time variation of soil temperature and specific humidity at the ground surface, a force restore method suggested by *Deardorff* [1978] was employed for bare ground condition.

4. Result and Discussion

4.1. Concentrations of NO, NO_2, SO_2 and CO in case of no wind storm

Kangnung city is located at the coastal line, which lies from south to north-west. Fig. 3 shows the hourly variations of NO (ppb) measured at Kangnung environmental observation point [*WREA*, 1994] from March 26 through 28, 1994, under the prevailing of strong synoptic-scale westerly winds. On March 26, 1994, before occurrence of a windstorm, the moderate synoptic scale westerly winds blew over the north-eastern Asian countries, especially China, Korea and Japan. However, at 1200 LST on March 27 in Fig. 1, the westerly winds became stronger and penetrated into the Korean peninsula, passing through eastern steep mountains in the west of Kangnung city and causing strongly enforced downslope windstorms along the lee side of the coastal mountains. The windstorm continued to pose until midnight of March 28, and the effect of the windstorm upon the coastal wind fields gradually decrease from March 29.

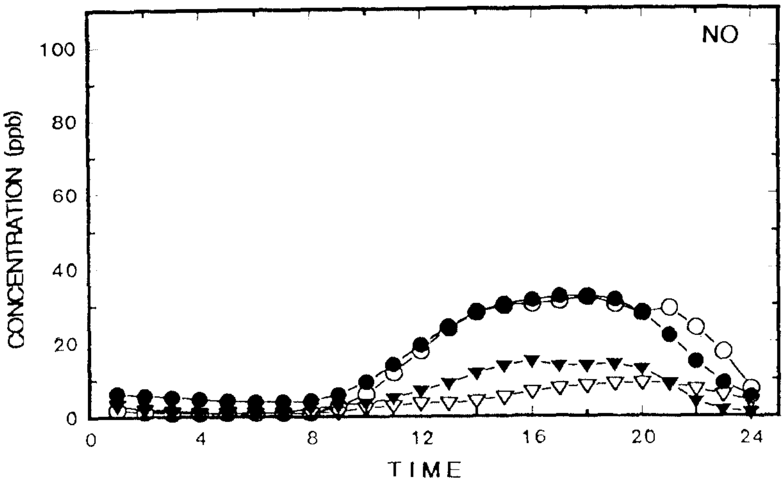

Fig. 3. Hourly concentration of NO (ppb) at Kangnung Environmental Observation Point. ○, ●, ▽, and ▼ mean March 26, 27, 28 and 29, 1994.

From 0100 LST to 0800 LST on March 26, before the storm period, the concentrations of NO at Kangnung city were in the range of 2.0 ppb ~ 1.0 ppb. After this time, that is, office hours during the day, their concentrations tend to be higher in the afternoon, until 1800 LST with magnitudes of 23.7 ppb to 32.0 ppb and gradually decrease to 7.3 ppb until midnight. Then, their concentrations remain constant before 0800 LST at the beginning of office hour on the next day morning, March 27. The hourly variation of NO concentration on March 29, after the storm period, has a similar pattern to that of March 26. Even if the NO concentrations are much lower magnitudes of 1.0 ppb to 15.0 ppb, they are still higher in the afternoon than at late night.

As we have already known, the largest NO_x contributors are the combustion of fuels from motor vehicle and heating apparatus [*Stephen*, 1969a, 1969b]. The NO_2 cocentrations in the range of 2.0 ppb ~ 51.7 ppb are also much higher in the daytime than nighttime, with a maximum value of 51.7 ppb at 2100 LST, showing a similar tendency of the NO distribution on the whole (Fig. 4). We may say that during the day, the NO and NO_2 concentrations at Kangnung would be sufficently controled by the emission amounts from automobiles in the office hours and heating fuel combustion concentrated in the urban area on cool and sunny day. Thus, the high concentrations NO and NO_2 on the ground level during the day and in the early evening should be attributed to the increase of emitted gases by automobiles and heating facilities.

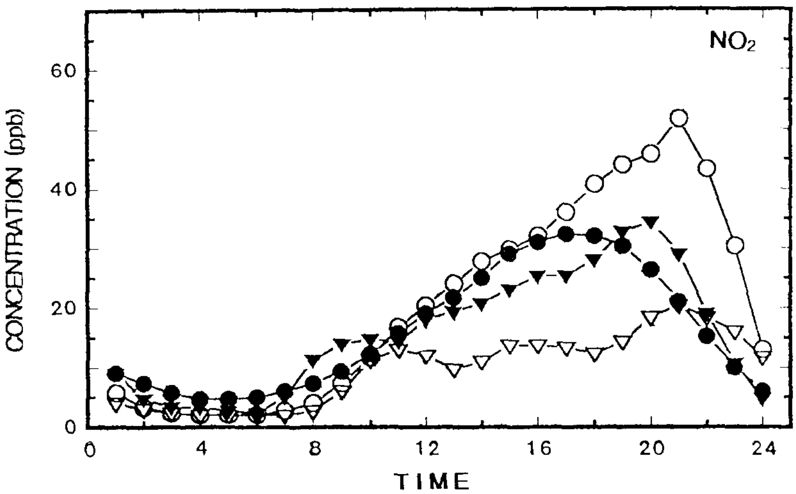

Fig. 4. Same as Fig. 3 except for NO_2 (ppb) at Kangnung Environmental Observation Point. ○, ●, ▽, and ▼ mean March 26, 27, 28 and 29, 1994.

Further consideration was given to meteorological conditions such as atmospheric circulations and stabilities over Kangnung city. When a westerly synotic-scale wind, during the day, blows over Mt. Taegwallyung and an easterly sea breeze generated by the meso-scale temperature contrast of air between inland and sea also approaches Kangnung city, these two different kinds of winds in the opposite directions are in the confront each other and air could be trapped by these wind systems, resulting in relatively weak surface winds. Thus, on March 26 or March 29, the NO concentrations during the day can also increase through the convergence of emitted nitric oxides emmited from mainly automobiles and partle heating fuel combustions by two opposite winds. Since we know that most of the nitrogen oxide emitted into the air from the combustion processes is NO, there must be oxidization process of NO to NO_2, resulting in some amount of increase of NO_2 during clear and sunny daytime, but as shown in Figure, the difference from NO_2 and NO concentrations denotes a little amount of oxidization.

On the other hands, at night after the returning time from office to home, the NO concentrations should be lower and lower due to gradually decrease of number of auto-vehicles on the street until middight and then, their concentrations remain nearly constant under emitted amount from ony a small number of running vehicles. After sunset, both existed westerly wind could be associated with westerly land breeze induced by a surface cooling from inland to sea and more intensified resultant wind could spread out the NO_x produced in the daytime or nighttime. So, the NO and NO_2 concentrations gradually decrease until midnight, and then remain in the almost constant and low magnitudes before sunrise. Since we could expect niether increase of NO and NO_2 by the emitted gases from auto-mobiles nor tapping by land breeze at night, the concentrations of NO and NO_2 were lower in the nighttime than daytime, remaining very low until early in the morning. Especially, the reason why the highest concentration of NO_2 at 2100 LST, after sunset, is largely due to a lot of spending of heating fuels such as oil by boilers in the resident area such as apartment complex and in part, vehicle fuel combustion. In most of apartments, the operation of the boiler occurs usually once in the evening rather than more times at the late night on clear and cool day in the spring season. As we have known that nitrogen oxides are produced by combustin of fuels in order of oil greater than gas, the NO_x concnetrations largely depend upon the amount of combustion of heating fuels after sunset on a still cool day at Kangnung city.

The general feature of diurnal variations of NO and NO_2 concentrations at Kangnung city is much different from the case of Los Angeles investigated by *Leighton* [1961], *Perkins* [1974] and *Stephens* [1969a and 1969b], as we known that after sunrise, the NO_2 concetration increses; the NO concetration decreases through a photochemical reaction of NO, NO_2 and O_3 processes. It seems that the NO and NO_2 concentrations at Kangnung city are affected by both combustion of auto-vehicle and heating boiler, but those at Los Angeles are due to the combustion of largely automobile fuel, because SO_2 concentrations at Kangnung are also found to be higher in the afternoon, until early evening.

Gases such as sulfur dioxide undergo a transformation in the atmosphere to particulates as sulfates or sulfuric acid droplets. Due to wind motion, the sulfur compounds emitted in a certain location can be removed from the atmosphere in the distance of hundred kilometers downwind. The SO_2 cocentrations, which are affected by primary heating fuel combustion in stationary source such as fuel oil and by secondly motor vehicle gasoline are also much higher in the daytime than nighttime, with maximum values of 76.7 ppb at 1700 LST and 82.7 ppb at 1600 LST, in the range of 7.7 ~ 73.3 ppb and have a slight different distribution of the NO and NO_x distributions, showing a similar tendency on the whole (Fig. 5). During the day, the SO_2 could be isolated by the confrontation of westerly synoptic wind with easterly sea breeze, enhancing the increase of SO_2 concentrations at the city. As nighttime went on, the enhanced surface winds associated with both westerly synoptic wind and land breeze drived out the existed SO_2 or the SO_2 emitted from small number of automobiles into the coastal sea, resulting in their low concentrations until early in the morning.

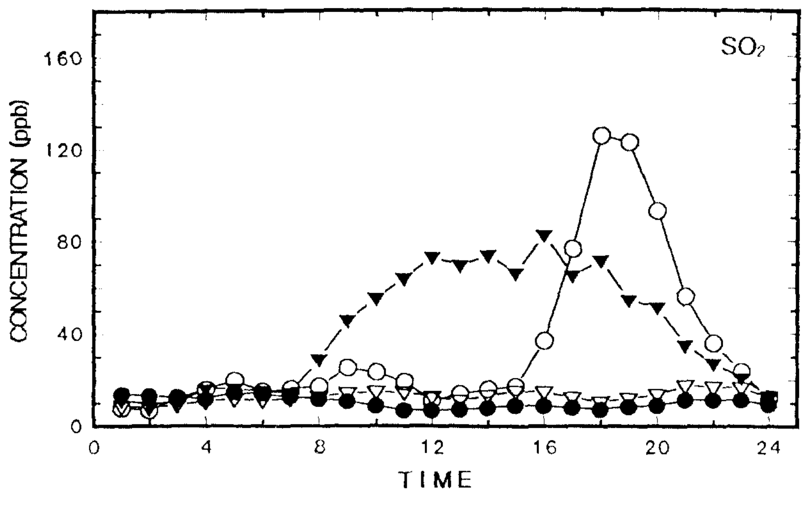

Fig. 5. Same as Fig. 3 except for SO_2 (ppb) at Kangnung Environmental Observation Point. ○, ●, ▽, and ▼ mean March 26, 27, 28 and 29, 1994.

As shown in Fig 6, the CO (carbon monoxide) concentrations with 30 ppm ~ 127 ppm are slightly higher for daytime ours until evening at 2100 LST than the rest of nighttime hours, but they are still not much changed all day long. Of course, the higher concentrations during the daytime are due to the emittion of gases from automoblies and heating favilities, under the partly influence of trapping of the air by sea breeze and the maximum concentration result from a great amount of the combustion of heating fuels in the cool evening near 21 LST. *Weinstock and Niki* [1972] indicates that natural sources of CO are some 10 times larger than the man-caused sources and man's activityies are not producing the majority of atmospheric CO. Even if the CO concentrations were not much changed at night, comparing to the daytime one, they were also spreaded out into the coastal sea by both westerly wind and land breeze, becoming lower and almost constant values.

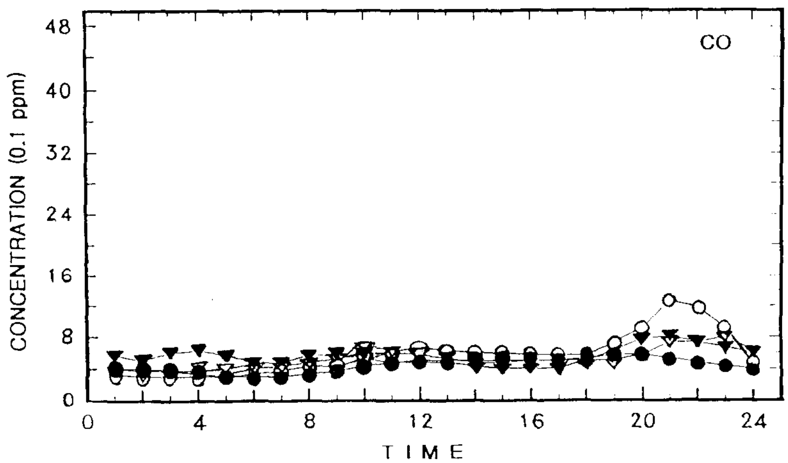

Fig. 6. Same as Fig. 3 except for CO (0.1ppm) at Kangnung Environmental Observation Point. ○, ●, ▽, and ▼ mean March 26, 27, 28 and 29, 1994.

4.2. During windstorm period

As a strong westerly wind blows over a high sloping Taegwallyang mountain (Mt. Whangbang: 1407m), it could be enforced into the formation of a windstorm with a speed more than 12m/s, passing through Kangnung and moving toward the East Sea. At the same time, easterly sea breeze approaches with a speed of 7m/s over the coastal sea to the inland of the Kangung coast. On March 27 at the beginning of the windstorm period, the NO has high concentration in the afternoon and low one at night. Strictly speaking, the NO concentrations increase from 0900 LST until 1800 LST and decrease until midnight. After midnight, they remain almost constant with very low magnitudes until 08 LST on the next day moring.

Even if the windstorm developed along the downslope of the mountain in the west side of Kangnung and produced relatively strong surface winds, the surface winds at the environmental point of the city were under the control of the sea breeze and the air could be isolated by both westerly internal gravity wave and easterly sea breeze in the opposit directions. So, we can see a similar pattern of the NO concentrations on March 27 to that of March 26 and the distribution of NO_2 concentrations also shows similar relation to that of March 26 with slightly lower magnitudes. The NO and NO_2 around 1700 LST have very high magnitudes of 32.3 ppb and 32.3 ppb, respectively.

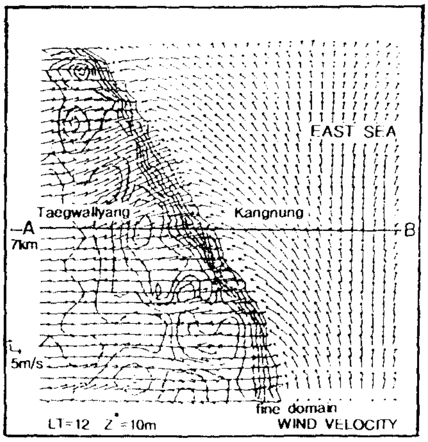

Fig. 7a. Surface winds (m/s) at 10m height near Kangnung city in a fine-mesh domain of the model at 12 LST, March 27, 1994.

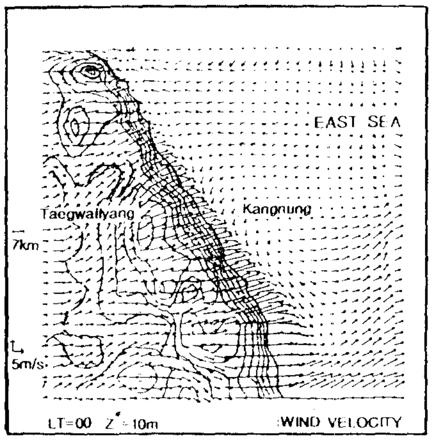

Fig. 7b. Same as Fig. 7a except for 00 LST, March 28, 1994.

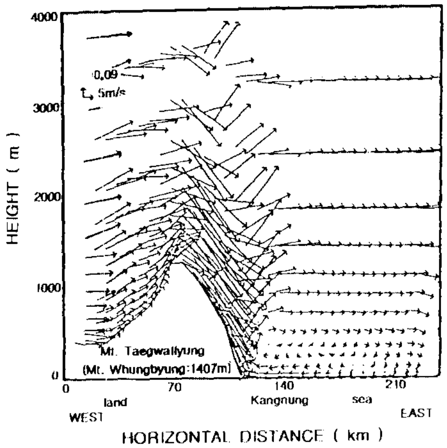

Fig. 8a. Vertical profiles of wind vector (m/s) on 15 levels over s straight cutting line (A-B) from Kangnung toward Mt. Taegwallyang at 12 LST, March 27, 1994.

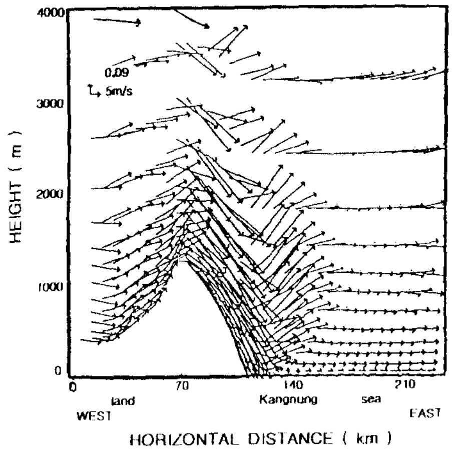

Fig. 8b. Same as Fig. 8a except for 00 LST, March 28, 1994.

At 1200 LST March 27, 1994, since these two different kinds of winds in the opposite directions are in the confront each other, the sea breeze confine to the downtown of Kangnung city and the surface winds near the ground at the edge of lee side of

Taegwallyang mountain, just west side of Kangnung was 12m/s, but the surface wind speeds with easterly in the Kangnung city take a range of 3m/s to 5m/s (Figs. 7a, 8a and 9a). Fig. 10a depicts the potential temperature deviation which substracts mean potential temperature of atmosphere in the model domain from potential temperature at each level of 15 levels. At 1200 LST on March 27, the upper atmosphere in the lee side of Mt. Taegwallyang was very stable and the subsidence of air from the upper layer toward 800m height over ground could be expected to occur, resulting in the distingtively development of downslope winds along the east slope of the mountain in the coastal region. An internal gravity wave generated by the intensified downslope winds bound up over a convective boundary layer induced by surface heating and sea breeze and blow over the coastal sea. From 1000 LST on March 27 until 2100 LST, the concentrations of NO and NO_2 rapidly increase with the magnitudes of 11.7 ppb to 51.7 ppb for NO_2 and 9.3 ppb to 21.7 ppb for NO.

In the nighttime, the eastward downslope winds, which could be intensified by momentum transfer from the strong upper level winds toward the surface due to nighttime stability such as moving down of subsidence inversion layer and the association of meso-scale land breeze from land toward the coastal sea could make one atmospheric circulation in the coastal region, and the NO and NO_2 gases were not converged by this wind regime(Figs. 7b, 8b, 9b, and 10b). Under this situation, the surface winds near the Kangnung city became very strong with over 18m/s as gust and the concentrations of NO and NO_2 at 00 LST March 28 were 3.3 ppb and 4 ppb lower than those of 2100 LST March 27 in not trapping situation, but dissipating by the strong winds.

During the daytime after 0900 LST March 28, two kinds of circulations, especially under the strong development of downslope winds should be produced again with the surface wind speed of 18 m/s at Kangnung city, and the concentrations of NO and NO_2 increase in the afternoon with maximum values of 8.7 ppb at 1900 LST and 13.7 ppb at 1700 LST. Especially, at 12 LST on March 28 under the more severe windstorm than on March 27, the NO and NO_2 concentrations are very low, showing almost half of those concentrations in cases of without windstorm, because the surface wind speed near Kangnung were over 15m/s and a large amount of the NO and NO_2 gases could be dissipated by the strong winds. From 2100 LST after sunset time, the NO and NO_2 concentartions remain almost constant under the strong downslope windstorm, similarly to the case of March 27. Otherwise, after 0700 LST on March 29, the NO concentration slightly increases again with the weak influence of the windstorm, but the NO_2 shows a similar pattern of March 26 with a slightly lower magnitudes.

The SO_2 concentrations from March 27 and 28 keep almost constant with very low magnitudes about 10 ppb, regardless daytime and nighttime, due to their dissipations by the strong surface winds. From 0800 LST on March 29, their concentartions depict the general distributions which have higher value in the afternoon and lower one at night.

Although we can expect that the SO_2 concentrations were also affected by the emitted amount of SO_2 through the combustion of automobile gasoline and heating oil and by sea breeze during the day, the SO_2 should be drived out into the coastal sea by the surface strong winds. At night, the emitted sulfur dioxide gases from auto-vehcle and heating facilities were not only small amount, but were dissipated by the winds.

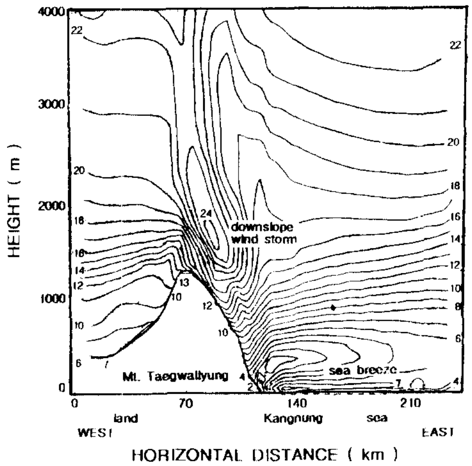

Fig. 9a. Vertical profiles of horizontal wind speeds (m/s) on 15 levels over a straight cutting line (A-B) from Kangnung toward Mt. Taegwallyang at 12 LST, March 27, 1994.

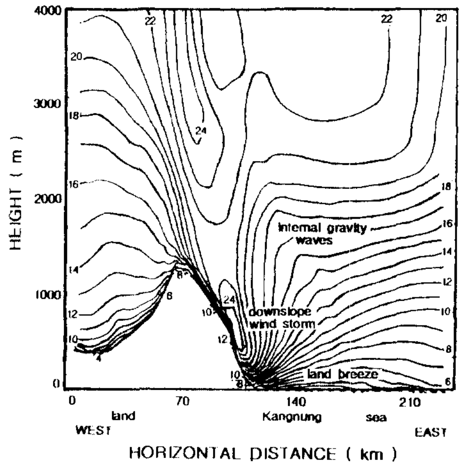

Fig. 9b. Same as Fig. 9a except for 00 LST, March 28, 1994.

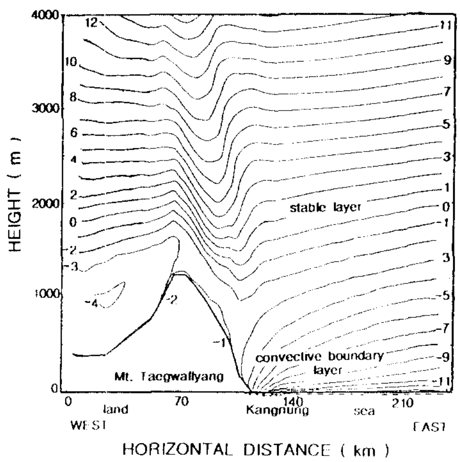

Fig.10a. Vertical profiles of potential temperature deviation (K) on 15 levels over a straight cutting line (A-B) from Kangnung toward Mt. Taegwallyang at 12 LST, March 27.

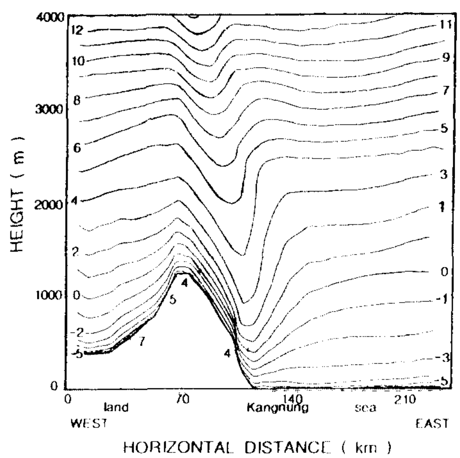

Fig.10b. Same as Fig. 10a except for 00 LST, March 28, 1994.

Similarly to the case of SO_2, the concentrations of CO during the storm period remain also constant, even if they show slightly higher magnitude during the day than at night. It means that they could be spreaded out by the strong surface winds which were induced by the downslope windstorm.

5. Conclusion

Diurnal variationos of NO, NO_2, SO_2 and CO concentrations were investigated from March 26 through 29, 1994 at Kangnung city. In case of no windstorm on March 26 and 29, the high concentrations of NO, NO_2, and SO_2 on the ground level were observed in the afternoon, especially near 1600 and 1800 LST, 2000 and 2100 LST, 1600 LST and 1800 LST, under a great amount combustion of motor vehicle and heating fuels, but their low concentrations at night were produced by small consumptions of vehicle and heating fuels. Under the confratation of westerly synoptic-scale winds blowing over the steep mountain and easterly meso-scale sea breeze during the day, these gases should be converged by two opposite winds and produce higher concentrations in the afternoon. In progress of nighttime, the association of existed westerly wind and land breeze can produce relatively strong winds and the strong surface winds dissipate some amount of gases, resulting in lower concentrations.

During the storm period, from March 27 through 28, the enforced westerly winds over the mountain generated a windstorm in the lee side of the mountain in the west of Kangnung, and westerly internal gravity waves with hydraulic jump motions, by the storm. At the same time, easterly meso-scale sea breeze streched out to the lower level of the eastern side of the mountain, as the eastward internal gravity waves interrupted the propagation of the sea breeze. As the encountering point of two opposite wind systems moved down to Kangnung area, NO and NO_2 were removed by the strong surface winds, to a great extent. Comsequently, their maximum concentrations are detected at 1800 LST and 2000 LST, 1700 LST and 2100 LST. Otherwise, at night, the windstorm could be strongly developed under the momentum tranfer from upper level toward the ground and it should produce very strong surface winds over 18 m. This strong surface winds easily dissipate the NO and NO_2 into other location. In particular, the SO_2 had very low concentrations during the storm period and it is very difficult to find their maximum concentrations, due to their removal by the strong surface. Hence, it is almost constant, regardless of daytime and nighttime. The CO concentrations were very slightly lower during the strom period than both before and after the storm periods. However, under the persistent strong surface winds, their concentrations were nearly constant without much changes, all day long.

Acknowledgements

The author would like to express their thanks to Mr. S. Takahashi and T. Hanfusa of Meteorological Research Institute, Japan Meteorological Agency, for their fruitful comments on meteorological data and model, and National Fisheries Research and Development Agency of Korea for oceanic data. This paper was supported in part by NON DIRECTED RESEARCH FUND, Korea Research Foundation, the Ministry of Education in 1995, under grant for "Variation of atmospheric pollution concentrations due to the development of internal gravity waves in Kangwondo coastal regions".

References

Businger, J. A., Turbulence transfer in the atmospheric surface layer, In Workshop on Micrometeorology (D. A. Haugen, ed), Amer. Meteor. Soc., pp.67-100, 1973.

Choi, H. and J. Choi, Characteristics of onshore winds in the coastal thermal internal boundary layer, *J. Korean Meteor. Soc.*, **30**, 1-11, 1994.

Choi, H. and J. Choi, Atmospheric pollutant concentrations under the influence of internal gravity wave and sea-land breeze circulations in the mountainous coastal regions, *Korean J. Geophys. Res.*, **23**, 18-33, 1995.

Choi, H., Three dimensional numerical modelling on the development coastal internal boundary layers in Cheju island, *J. Korean Meteor. Soc.*, **32**, 1-16, 1996.

Choi, H., Numerical modelling for air flows in the eastern mountainous coastal seas of Korea, *Lar Mer*, **34**, 133-148, 1996.

Davies, H. C., Observational studies and interpretation of the mountain pressure drag during ALPEX, in observation, theory and modelling of orographic effects, ECMWF, Reading, 113, 136pp. 1987.

Durran, D. R. and J. B. Klemp, Another look at downslope wind storms. Part II: Non linear amplication beneath wave overturning layers, *J. Atmos. Sci.*, **44**, 3402-3412, 1987.

Deardoff, J. W., Efficient prediction of ground surface temperature and moisture with inclusion of a layer of vegetation, *Geophys. Res.*, **38**, 659-661, 1978.

Friehe, C. A. and C. D. Winant, Observation of wind and sea surface temperature structure off of the northern California coast, *Proceeding of 1st International Conference on Meteorology and Air/Sea Interaction of the Coastal Zone*, Hague, Amer. Meteor. Soc., pp. 209-214, 1982.

Hsu, S. A., Mesoscale nocturnal jetlike winds within the planetary boundary layer over a flat open coast, *Boundary-Layer Meteor.*, **17**, 485-494, 1979.

Hsu, S. A., Research in the coastal meteorology: basic and applied, *Proceeding of 2nd Conference on Coastal Meteorology*, Los Angles, Amer. Meteor. Soc., pp.1-7, 1980.

Hsu, S. A., Coastal Meteorology, Academic Press, 260pp. 1988.

Kimura, F., A numerical simulation of local winds and photochemical air pollution(I): two-dimensional land and sea breeze, *J. Meteor. Soc. Japan*, **61**, 862-878, 1983.

Kuwagata, T. and M. Sumioka, The daytime PBL heating process over complex terrain in central Japan under fair and calm weather conditions. Part III: Daytime thermal low and nocturnal thermal high, *J. Meteor. Soc., Japan*, **69**, pp.91-104, 1991.

Kimura, F. and S. Takahashi, The effects of land-use and anthropogenic heating on the surface temperature in the Tokyo metropolitan area: numerical experiment, *Atmospheric Envir.*, **25**, 155-164, 1991.

Klemp, J. B. and D. R. Durran, An upper condition permitting internal gravity wave radiation in numerical mesoscale models, *Mon. Wea. Rev.*, **111**, 430-440, 1983.

Leighton, P. A., *Photochemistry of air pollution*, Academic Press, New York, pp.10-65, 1961.

Lilly, D. K., J. M. Nicholls, R. M. Chervin, P. J. Kennedy and J. B. Klemp, Aircraft measurements of wave momentum flux over the Colorado Rocky Mountains, *Q. J. R. Meteor. Soc.*, **108**, 625-642, 1982.

McPherson, R. D., A numerical study of the effect of a coastal irregularity on the sea breeze, *J. Appl. Meteor.*, **9**, 767-777, 1970.

Mellor, G. L. and T. Yamada, A hierachy of turbulence closure models of planetary boundary layers, *J. Atmos. Soc.*, **31**, 1791-1805, 1974.

Monin, A. S., The atmospheric boundary layer, *Annual Review of Fluid Mechanics*, **2**, 225-250, 1970.

NFRDA, Analyzed NOAA satellite picture on the sea surface temperature in the East Sea (Japan Sea), National Fisheries Research and Development Agency, 1994.

Orlanski, I., A simple boundary condition for unbounded hyperbolic flows, *J. Comp. Phys.*, **21**, 251-269, 1976.

Panofsky, H. A. and Dutton, J. A., *Atmospheric Turbulence*, John & Wiley, New York, pp.1-100, 1984.

Paulson, C. A., The mathematical representation of wind speed and temperature profiles in the unstable atmospheric surface layer, *J. Appl. Meteor.*, **9**, 857-861, 1970.

Perkins, H. C., *Air Pollution*, McGraw Hill, pp.1-407, 1974.

Peltier, W. R. and T. L. Clark, The evolution and stability of finite amplitude mountain waves. Part II: Surface wave drag and severe downslope windstorms, *J. Atmos. Sci.*, **36**, 1498-1529, 1979.

Pielke, Roger A., *Mesoscale meteorological modeling*, Academic Press, 612pp. 1984.

Plate, E. J., Aerodynamic characteristics of atmospheric boundary layers, pp. 1-190, U. S. Atmospheric Energy Commission, 1971.

Raynor, G. S., S. SethuRaman and R. M. Brown, Formation and characteristics of coastal internal boundary layer during onshore flows, *Boundary Layer Meteor.*, **16**, 4587, 1979.

Satomura, T. and P. Bougeault, Orographic wave drag during PYREX experiment, *Proceeding of Spring Meeting of the Meteorological Society of Japan*, Tsukuba, pp.1-282, 1992.

SethuRaman, S., Observation of the bounadry layer wind structure near land-sea interface, *Proceeding of 1st International Conference on Meteorology and Air/Sea Interaction of the Coastal Zone*, Hague, Amer. Meteor. Soc., pp.4-7, 1982.

Smith, R. B., A measurement of mountain drag, *J. Atmos. Sci.*, **35**, 1644-1654, 1978.

Smith, R. B., Hydrostatic airflow over mountains, *Adv. Geophys.*, **31**, 1-41, 1989.

Smolarkiewicz, P. K. and R. Rotunno, Low Froude number flow past three dimensional obstacles. Part I: Baroclinically generated lee vortices, *J. Atmos. Sci.*, **46**, 1154-1164, 1989.

Stephene, E. R., Photochemistry of smog, *California Air Environ.*, 11-52, 1969a.

Stephene, E. R., Chemistry of atmospheric oxidants, *J. Air Pollution Control Assoc.*, **19**, 181-185, 1969b.

Taylor, P. A., A model of airflow above changes in surface heat flux, temperature and roughness for neutral and unstable conditions, *Boundary-Layer Meteor.*, **1**, 18-39, 1970.

Weinstock, B. and H. Niki, Carbon monoxide balance in nature, *Science*, **176**, 212, 1972.

Williams, R. G., A procedure for wind field construction from measured data which utilizes local surface roughness, *Proceeding of 2nd Conference on Coastal Meteorology*, Los Angles, Amer. Meteor. Soc., pp.1-307, 1980.

WMO, Scientific results of the Alpine experiment, GARP publication series, 27, WMO, Geneva, pp. 1-50, 1986.

WREA, Observation data of nitrogen oxides, ozone, total suspended particle, 1994.

Yamada, T., Simulation of nocturnal drainage flows by a q^2-l turbulence closure model, *J. Atmos. Sci.*, **40**, 91-106, 1983.

Yamada, T. and G. L. Mellor, A numerical simulation of the BOMEX data using a turbulence closure model coupled with ensemble cloud relations, *Q. J. R. Meteor. Soc.*, **105**, 95-944, 1983.